



PROGRESS REPORT

PROJECT TITLE: Corn derived materials
PROJECT NUMBER: 1088-18EU
REPORTING PERIOD: January 1 – March 31, 2019
PRINCIPAL INVESTIGATOR: Marc Hillmyer
ORGANIZATION: University of Minnesota
PHONE NUMBER: 612-625-7834
EMAIL: hillmyer@umn.edu

1.) PROJECT ACTIVITIES COMPLETED DURING THE REPORTING PERIOD. (*Describe project progress specific to goals, objectives, and deliverables identified in the project workplan.*)

The goal of the project led by Frank Bates and Chris Ellison is to toughen intrinsically brittle poly(lactide) (PLA) by the addition of small quantities of block copolymer (BCP). A BCP contains two different polymers joined by a covalent bond; in this work a rubbery polymer block to toughen PLA and another polymer block that is chemically compatible with PLA to aid in dispersion. In previous quarters we described blending several different diblock copolymers and the resulting mechanical properties. In the last quarterly report, we have described an increase in toughness of commercial PLA without signs of physical aging over more than a month at room temperature upon the addition of 5 wt.% of the diblock copolymer poly(butylene oxide)-b-poly(ethylene oxide) (PBO-PEO). This compound, with number average molecular weight $M_n = 7,000$ g/mol and containing 35 wt.% PEO, is available from Olin Chemical under the tradename Fortegra™ 100. During the past quarter we extended this investigation and probed the underlying deformation mechanism responsible for this remarkable behavior.

PLA is known to deform by crazing,¹ which leads to the formation of a network of fine cracks separated by load bearing fibrils that are spaced apart by approximately 5-30 nm.¹ The creation of a craze is associated with energy absorption during fibril formation, which inhibits crack propagation and results in a tough plastic. However, if the craze fibrils begin to fail, the fine cracks will coalesce and result in larger cracks that will lead to macroscopic failure. Crazing is both a toughening mechanism, and a precursor to failure. As a result, the crazing mechanism in PLA needs to be understood to effectively control toughening this material. To investigate crazing at the fibril length scale, small angle x-ray scattering (SAXS) has been employed.

The overarching objective of the project led by the Dauenhauer group is to design catalysts to selectively produce C4/C5 dienes at rates comparable to typical industrial processes, using feedstocks which can be derived from lignocellulosic-biomass (e.g. corn). In the past quarter, we have worked on detailed kinetics of the dehydra-decyclization of biomass-derived cyclic ether 2-methyltetrahydrofuran (2-MTHF) to C5 linear dienes, providing valuable new insights into this chemistry. Specifically, we evince the role of acidic site strength and the void-sizes of the sub-nanometer pores that these transformations take place, on the activity and selectivity to produce dienes. In the process, we also highlight a rigorous paradigm of studying weakly acidic materials under reaction conditions and comparing the stability of different classes of

materials with widely different reactivities. Finally, combining these insights, we report a high (~85%) yield to 1,3-Pentadiene, which is significantly higher than previously reported values.²

2.) IDENTIFY ANY SIGNIFICANT FINDINGS AND RESULTS OF THE PROJECT TO DATE.

The microscopic modes of deformation in PLA and PLA/PBO-PEO blends were examined by SAXS at different degrees of extension during tensile tests. The samples were molded into films in the melt state (130 °C) and quenched to room temperature. Dogbone shaped specimens were cut from the film in accordance with ASTM 1708 and tested at room temperature using an extension rate of 10 mm/min. The tests were terminated before failure at specified strains, so the samples could be investigated with SAXS, conducted at the Characterization Facility at the University of Minnesota using a SAXSLab Ganesha instrument with a CuK α x-ray source ($\lambda = 1.54 \text{ \AA}$) and a position sensitive Eiger 1 M detector. Three different types of samples were analyzed: i) “tough” neat PLA (aged < 2 hrs.) (Figure 1); ii) “brittle” neat PLA (aged > 24 hrs.) (Figure 2); and iii) PLA/PBO-PBO blends (aged for 2 days) (Figure 3). The geometry and orientation of the tensile experiment with respect to the SAXS patterns is shown in Figure 1. The 90° and 0° axes in Figure 1 are referred to as the meridional and equatorial axes, respectively, where the sample is stretched parallel to the meridional axis. A representative stress-strain curve obtained from freshly molded PLA is shown in Figure 1 along with SAXS patterns obtained at 3 different states of strain indicated by the colored symbols; the SAXS intensities have been normalized by the sample thickness.

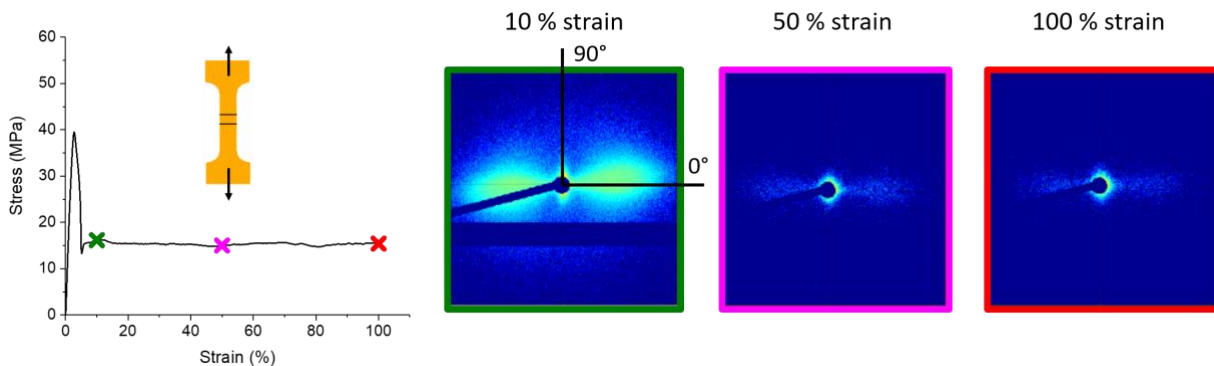


Figure 1. The left image is a tensile stress-strain curve of “tough” neat PLA (aged < 2 hrs.), where the different X symbols correspond to the strain at which the tests were terminated and the material was subsequently analyzed by SAXS. The right images are 2-D SAXS patterns at specified strains, where the samples were stretched in the vertical direction.

The pattern at 10 % strain shows intense equatorial and meridional scattering, due to crazes within the polymer matrix. But as the PLA specimen is further strained the equatorial scattering intensity decreases dramatically as revealed by the 50 % and 100 % strain 2-D patterns. This is most likely a result of the fine cracks coalescing as the fibril separating them break. The cracks will thus grow in size resulting in the fibrils being spaced further apart than what can be detected by SAXS. All the crazes that are observed in PLA appear to form by 10 to 50 % strain according to the 2-D SAXS patterns.

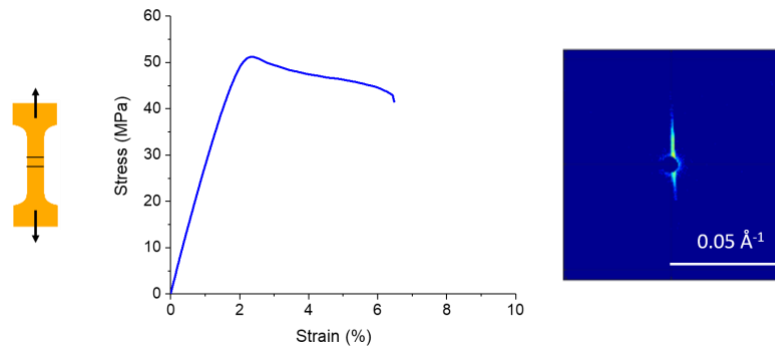


Figure 2. The left image is a tensile stress-strain curve of “brittle” neat PLA (aged > 2 days). The right image is a 2-D SAXS pattern, where the sample was stretched in the vertical direction until failure.

The pure molded PLA behaves very differently after aging for 24 hours. The 2-D SAXS pattern for “brittle” neat PLA exhibits only a meridional streak at failure, which is indicative of void formation while no scattering is observed in the equatorial axis, indicating no craze formation. Although void formation is a precursor to crazes, in the case of “brittle” PLA, the voids must have grown large, presumably due to unstable crazes, leading to crack propagation and failure at small strain.

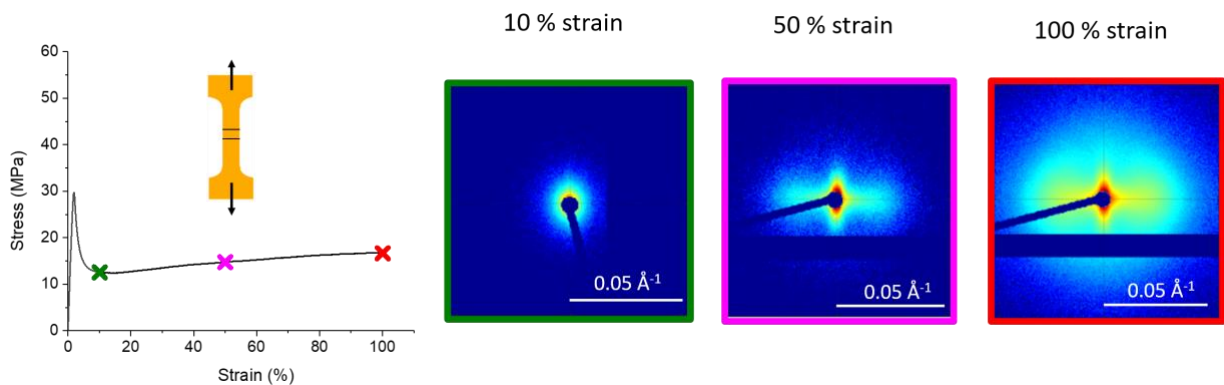


Figure 3. The left image is a tensile stress-strain curve of PLA/PBO-PBO blend (aged for 2 days), the different X symbols correspond to the strain at which the tests were terminated and the material was subsequently analyzed by SAXS. The right images are 2-D SAXS patterns at specified strains, where the samples were stretched in the vertical direction.

In contrast, to the “tough” and “brittle” PLA samples, the PLA/PBO-PEO blend behaves much differently as shown in Figure 3. At 10 % strain, the 2-D SAXS pattern intensity is relatively uniform at all azimuthal angles with a slight increase along the meridional axis. While the absence of equatorial lobes indicate absence of craze formation, the high intensity observed in the 2-D pattern suggests there is uncorrelated void formation. At 50 % strain, the intensity in both the equatorial and meridional axes increases, and the presence of two clearly defined lobes signifies craze formation. Subsequently at 100 % strain, the scattering intensity increases again in both the equatorial and meridional axes indicating additional crazes have formed compared to the 50 % strain sample.

That the scattering intensity continues to increase along both axes as the PBO-PEO/PLA sample is increasingly strained indicates that crazes are continually forming/propagating throughout this process. The addition of just 5 wt.% PBO-PEO to PLA leads to continual craze formation as the polymer is strained, and the crazes appear to be stable without coalescence of the fibrils after 2 days of aging. Moreover, we have discovered that this material remains tough after more than 46 days at room temperature. This is in strong

contrast to what is observed in freshly molded “tough” PLA. Also, according to the stress-strain curve in Figure 1 the stress remains constant at 15 MPa during extension of the “tough” neat PLA. As previously stated, there appears to be no new craze formation between 10 % strain and 100 % strain. Therefore, the stress required to craze the freshly molded pure PLA must be greater than 15 MPa. In comparison, for the PLA/PBO-PEO blend, (stress-strain curve in Figure 3) there is initial craze formation at 13 MPa. Addition of the BCP appears to lower the stress required for craze formation/propagation, which results in continued craze formation during stretching even after aging the material.

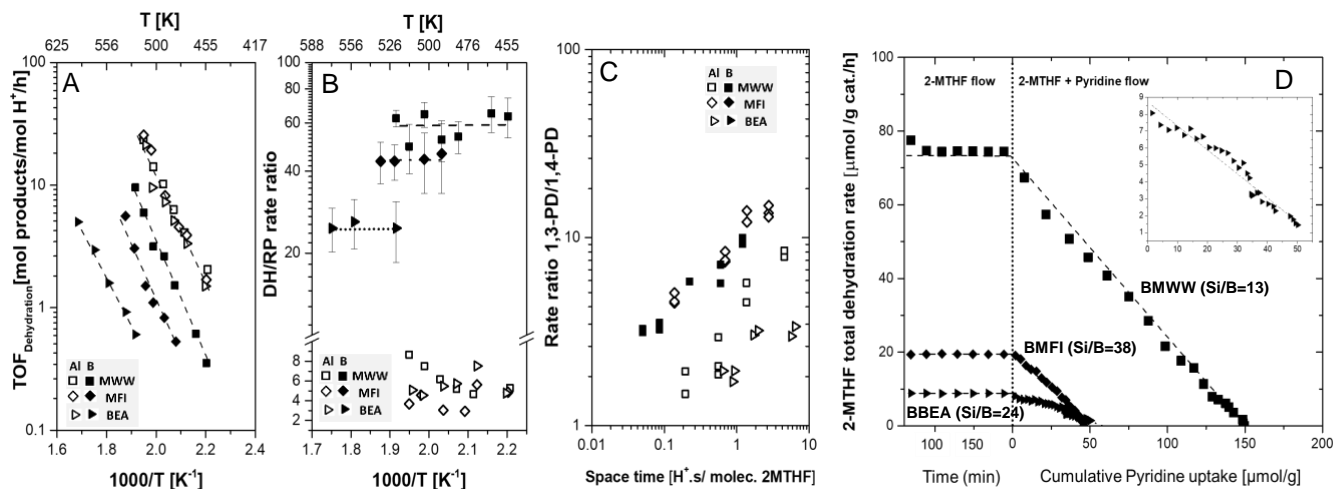
In the future, we will explore the morphology of PBO-PEO in PLA and its effects on the ability of the PLA matrix to craze. We suspect that the differences in 2-D SAXS patterns along with mechanical properties between PLA and PLA/PBO-PEO blend are related to the morphology of PBO-PEO in PLA. We hypothesize that PEO-PBO forms nanosized dispersions in the PLA. These dispersions can act as crazing initiation sites, either due to cavitation of the dispersion or due to differences in the compliance between the dispersion and the matrix (i.e. PLA). Either way, the dispersion or cavitated hole will act as a stress concentrator leading to void formation and crazing at lower stresses.

The Dauenhauer group has previously shown that weakly acidic phosphorus-containing zeolites show high (>90%) selectivities for corresponding dienes from the dehydro-decyclization of tetrahydrofuran (THF) and 2-methyltetrahydrofuran (2-MTHF), respectively.^{3,4} Due to a lack of understanding about the nature of active sites in these materials, our past efforts have instead focused on the synthesis and characterization of well-known weak Brønsted acidic borosilicates in three distinct zeolite frameworks (MWW, MFI, and BEA) to probe this chemistry. To deconvolute the effect of different heteroatoms and extents of confinement, aluminosilicates with the same three frameworks were also either synthesized or purchased.

Apparent kinetic measurements in the temperature range 453-573K showed that borosilicates catalyze the dehydration pathway at rates which are at-least ~5x lower than aluminosilicates (**Figure 4A**). However, the suppression in the competing pathway, namely, Retro-Prins (RP) condensation, on these materials is higher than the suppression of dehydration (DH) pathway, leading to higher dehydration selectivities for the weakly acidic borosilicates (**Figure 4B**), providing evidence that the origin of selectivity-control between dehydration and Retro-Prins pathways is strictly kinetic.

Reporting rates per active site (commonly called “turnover frequencies”) has proven to be challenging on weakly acidic materials like borosilicates,⁵ mostly due to heterogeneity of these sites as well as their dynamic nature dependent on the extent of hydration. While we use an ex-situ technique (¹¹B MAS NMR) to study the anchoring of boron in the framework, the number of protons catalyzing the reactions are best studied *in-operando*. In this work, we use *in-situ* pyridine titration during 2-MTHF dehydro-decyclization to estimate the number of Brønsted acid sites catalyzing the reaction. All the three borosilicates have sites which can protonate pyridine, and interestingly, the number of protons doesn't linearly correlate with the boron content of the materials (**Figure 4D**). The result suggests the ability to retain B inside the framework

Figure 4 a) Arrhenius plots for the apparent kinetics of dehydration on different catalysts; b) The variation of Dehydration/Retro-Prins rate ratio with temperature; and c) The variation of 1,3-Pentadiene/1,4-Pentadiene rate ratio with the reactor space times (Reaction conditions for A and B: $p_{2\text{MTHF}}=10.5$ torr, $\text{WHSV}=1.1\text{-}12.9$ h^{-1} , $X_{2\text{-MTHF}}<12\%$; for C: $T=503$ K, $p_{2\text{MTHF}}=2\text{-}110$ torr) d) In-situ Pyridine titration during 2-MTHF dehydrat-decyclization (Reaction conditions: $T=453\text{-}478\text{K}$, $p_{2\text{MTHF}}=4.5\text{-}10.5$ torr, Carrier gas flowrate= $40\text{-}60$ sccm, $X_{2\text{-MTHF}}<0.5\%$)



under reaction conditions is dependent on the zeolite topology, which further illustrates the need to study these sites *in-operando* conditions.

Another challenge to selectively produce the conjugated 1,3-Pentadiene (1,3-PD) is the production of the non-conjugated 1,4-Pentadiene (1,4-PD) during this process. Double-bond isomerizations are usually equilibrium-limited, but we show that the diene distribution remains far from equilibrium under our reaction conditions, and hence can be altered using kinetic parameters like reactor residence times (**Figure 4C**). Moreover, our data also shows the lack of any correlation between heteroatom identity and diene distributions, which likely means that even the weakly acidic borosilicates can effectively isomerize the double bond, and the reaction can be directed to the thermodynamically more stable 1,3-Pentadiene by merely controlling the contact-times. While the ratio of 1,3-PD/1,4-PD is likely dictated by many factors like crystallite sizes, density and proximity of protons, and diffusivities of these species in 10-member ring (10-MR) channels vs 12-member ring (12-MR) channels, our data at the very least suggests that the diffusivities of these species, and in turn the diene distributions can be successfully altered by using small 10-MR channels in catalysis as evidenced by the low 1,3-PD/1,4-PD rate ratio in 12-MR BEA across different reactor residence times.

Combining these two approaches, namely, *a*) utilizing weakly acidic borosilicates to suppress Retro-Prins condensation pathway, and *b*) using tighter confinement in 10-MR to enhance the isomerization of 1,4-Pentadiene to 1,3-Pentadiene, we report ~85% 1,3-Pentadiene yield at complete conversion of 2-MTHF on BMWW, and this performance is sustained for >100 hours on-stream, albeit under very low space velocity and high temperatures (~0.1 g 2MTHF/g cat./h, $T=658$ K).

Current work on this project involves a rigorous comparison of stability of both classes of materials (boro-, and aluminosilicates). Due to their vastly different reactivities, a simple time-on-stream comparison provides an incomplete picture, as aluminosilicates turn-over many more catalytic cycles than borosilicates per unit time. Moreover, the deactivation of both materials happens over widely different timescales, and a simple comparison of product selectivities at different times can also be misleading. We use total turnover numbers during the catalyst lifetime to establish the stability of these materials. Moreover, with the same

initial conversions, we look at product selectivities as a function of the fraction of total turnovers for these materials to rigorously compare the performance of the materials under industrially relevant conditions.

3.) CHALLENGES ENCOUNTERED. (*Describe any challenges that you encountered related to project progress specific to goals, objectives, and deliverables identified in the project workplan.*)

None

4.) FINANCIAL INFORMATION (*Describe any budget challenges and provide specific reasons for deviations from the projected project spending.*)

None

5.) EDUCATION AND OUTREACH ACTIVITIES. (*Describe any conferences, workshops, field days, etc attended, number of contacts at each event, and/or publications developed to disseminate project results.*)

None

¹Kramer, E. J. In *Microscopic and molecular fundamentals of crazing*, Berlin, Heidelberg, Springer Berlin Heidelberg: Berlin, Heidelberg, 1983; pp 1-56.

² *ACS Catal.* 2017, 7, 5248–5256

³ *ACS Sustainable Chem. Eng.* 2017, 5, 3732–3736

⁴ *ACS Catal.* 2017, 7, 1428–1431

⁵ *Ind. Eng. Chem. Res.* 2018, 57, 6673–6683